Journal of Applied Physics

Configuration of heat sources or sinks in a finite volume

J. Jung, S. Lorente, R. Anderson, and A. Bejan

Citation: J. Appl. Phys. **110**, 023502 (2011); doi: 10.1063/1.3610387
View online: http://dx.doi.org/10.1063/1.3610387
View Table of Contents: http://jap.aip.org/resource/1/JAPIAU/v110/i2
Published by the American Institute of Physics.

JOURNAL OF APPLIED PHYSICS **110**, 023502 (2011)

Configuration of heat sources or sinks in a finite volume

J. Jung,[1,2] S. Lorente,[3] R. Anderson,[4] and A. Bejan[1,a)]
[1]*Department of Mechanical Engineering and Materials Science, Duke University, Durham, North Carolina 27708-0300, USA*
[2]*Department of Mechanical Engineering, Korea Advanced Institute of Science and Technology, Daejeon, 305-701, Republic of Korea*
[3]*Laboratoire Matériaux et Durabilité des Constructions, Université de Toulouse; UPS, INSA; LMDC, 135, Avenue de Rangueil, F-31 077 Toulouse Cedex 04, France*
[4]*National Renewable Energy Laboratory, 1617 Cole Blvd., Golden, Colorado, 80401-3305, USA*

(Received 19 April 2011; accepted 28 May 2011; published online 19 July 2011)

This work documents the design method of allocating channels that serve as heat sources or heat sinks in a conducting body. First, we develop a numerical model to find the optimum channel spacing for specified properties of the surrounding medium, the time scale of the heat transfer process, and the dimensions of the configuration. Second, we show with scale analysis that the optimal spacing (S/D) must equal $\tau^{1/2}$ in an order of magnitude sense, where τ is the dimensionless time scale of the process. This conclusion holds for the two heat transfer histories that were considered, exponential and top hat. We extend the method to a packing of channels of two sizes (diameters and heat source strengths). The optimal spacings and packing density obey the scaling rule determined for packing sources of a single size. © *2011 American Institute of Physics*. [doi:10.1063/1.3610387]

I. INTRODUCTION

In this paper we consider the fundamental problem of how to position in a conducting body several parallel lines that serve as heat sources or heat sinks. The volume of the conducting body is finite. The objective is to distribute the lines in such a way that the overall thermal resistance between the volume and the sources is minimal. This means that when the heat generation rate is specified, the peak temperature difference between sources and volume should be minimal. Conversely, when the peak temperature difference is specified, the heat transfer rate between the lines and the finite volume should be maximal, i.e., the design represents the highest density of heat deposition in the volume, or heat extraction from the volume.

This fundamental problem has several important applications most notably in the design of heat pumps with heat extraction or release through pipes buried in the ground,[1–3] and the positioning of decaying nuclear waste underground.[4] In all such applications, the heat transfer interaction between the line sources (or sinks) and the ground is time dependent, for two reasons: transient heat conduction in the surrounding medium and the finite lifetime t_c of the line sources. For example, during heat pump operation the lifetime is dictated by the daily cycle and the seasonal weather variations. In nuclear waste storage, the lifetime is controlled by the decay of the heat generation rate.

As background for the method, we note that the phenomenon of design generation and evolution in nature and engineering is accounted for by the constructal law.[5] Design can be predicted and pursued based on principle.[6] In heat transfer, spacings have been determined based on constructal design for a high-density packager of plates, tubes, and other components in steady natural or forced convection.[6–11] In this paper, we consider the time-dependent counterpart of the search for high-density arrangements of line heat sources or sinks. The objective is fundamental, and consists of determining the relation between the line spacing, the time scale of the heat transfer process (t_c), the dimensions of the configuration, and the properties of the conducting ground.

II. MODEL

Assume that heat sources are positioned as several parallel thin cylinders, which are viewed in the cross section area A shown in Fig. 1. The third dimension is perpendicular A, and is aligned with the horizontal direction shown in the lower part of Fig. 1. The volume is fixed. Each heat source generates heat in time dependent fashion. The cylinders have the diameter D and are indicated by black discs. Because the available volume is finite, the boundary of A is modeled as insulated. In general, the number of cylinders and their placement on A are free to vary. The initial temperature of the surrounding medium is uniform, T_0. For simplicity, the effects of convection, phase change and heterogeneity are assumed negligible.

To start, we assume that the time scale of the heat interaction is t_c, and every cylinder generates heat according to the time-dependent behavior sketched in Fig. 2,

$$q(t) = q_0 \exp(-t/t_c), \tag{1}$$

where t is the time, and q_0 is the heat generation rate at $t = 0$. Later we will consider the step-change q(t) shown in Fig. 2. The release of heat creates a time-dependent temperature field over the domain A. All the thermophysical properties of the surrounding medium are assumed to be constant.

[a)]Author to whom correspondence should be addressed. Electronic mail: abejan@duke.edu.

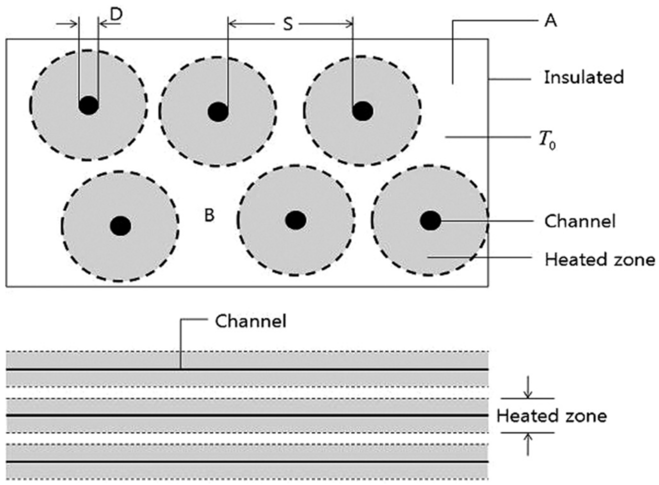

FIG. 1. Conducting finite-size volume with several embedded line heat sources or sinks.

III. NUMERICAL FORMULATION

The heat transfer is by conduction and is governed by the equation for energy conservation,

$$\rho c \frac{\partial T}{\partial t} = k\left(\frac{\partial^2 T}{\partial x^2} + \frac{\partial^2 T}{\partial y^2}\right), \tag{2}$$

where ρ, c, k, and T are the density, specific heat, conductivity, and temperature of the conduction medium. Dimensional variables are defined by writing

$$x^* = \frac{x}{D}, \quad y^* = \frac{y}{D}, \quad t^* = \frac{t}{t_c}, \quad \theta = \frac{T - T_0}{T_m - T_0}, \tag{3}$$

where T_m is the allowable ceiling temperature for the conducting medium. This means that the value of θ cannot exceed 1. When Eq. (2) is transformed by using Eqs. (3), the conduction equation becomes

$$\frac{1}{\tau}\frac{\partial \theta}{\partial t^*} = \frac{\partial^2 \theta}{\partial x^{*2}} + \frac{\partial^2 \theta}{\partial y^{*2}}, \tag{4}$$

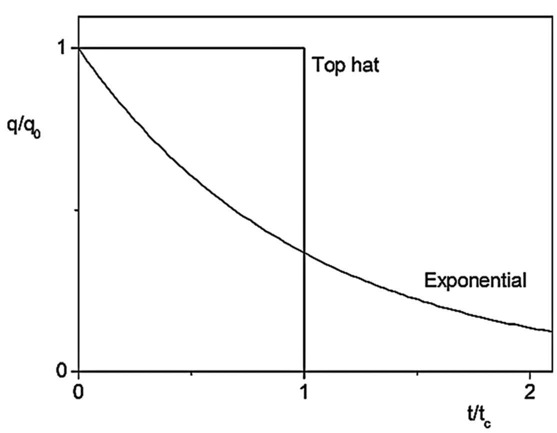

FIG. 2. Two kinds of time-dependent behavior of the heat generation rate with the same time scale, t_c.

where τ is the dimensionless lifetime of the heat generation process,

$$\tau = \frac{\alpha t_c}{D^2}, \tag{5}$$

and α is the thermal diffusivity of the medium. The cylinders are numerous, equidistant, and arranged in a square pattern that covers the computational domain shown in Fig. 3. The initial and boundary conditions are

$$k\left(\frac{\partial \theta}{\partial n}\right) = 0 \text{ on } \Gamma_1, \tag{6}$$

$$k\left(\frac{\partial \theta}{\partial n}\right) = q''(t^*) \text{ on } \Gamma_2, \tag{7}$$

$$\theta = 0 \text{ at } t^* = 0, \tag{8}$$

where Γ_1 and Γ_2 are the boundaries of computational domain and the boundary of cylinders that generate or absorb heat.

The conduction equation, boundary conditions, and initial condition were discretized by the finite-difference method. The nondimensional temperature field was determined numerically using the explicit method.[12] In order to increase the numerical accuracy, the step size and the grid size ($\Delta t^*, \Delta x^*, \Delta y^*$) were decreased until the value of

$$\left|\frac{\theta^{old}(t^*, x^*, y^*) - \theta^{new}(t^*, x^*, y^*)}{\theta^{old}(t^*, x^*, y^*)}\right|$$

was less than 0.01. In present numerical simulations we used $\Delta t^* = 10^{-5}, \Delta x^* = \Delta y^* = 10^{-3}$.

We validated the numerical solution further by comparing the temperature distributions obtained from the numerical model with the analytical solution for the temperature variation in the vicinity of a line heat source with constant heat generation rate[13]

$$\theta(r,t) = \frac{q'}{4\pi k}\int_{r^2/4\alpha t}^{\infty} \frac{e^{-u}}{u} du, \tag{9}$$

where q' is the constant source strength, i.e., the heat generation rate per unit of length of line heat source. At sufficiently long times and small radial distances such that $r^2/4\alpha t$ is smaller than 1, the temperature distribution approaches

$$\theta(r,t) \cong \frac{q'}{4\pi k}\left[\ln\left(\frac{4\alpha t}{r^2}\right) - 0.5772\right]. \tag{10}$$

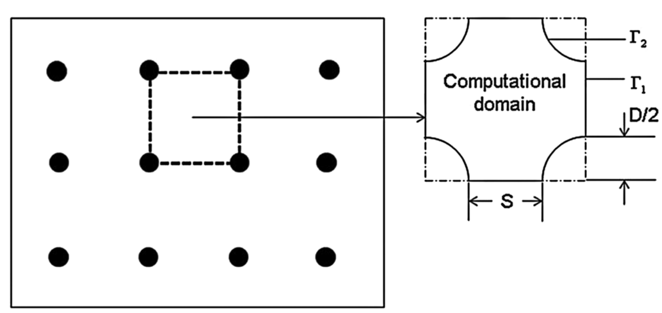

FIG. 3. Computational domain and boundary conditions.

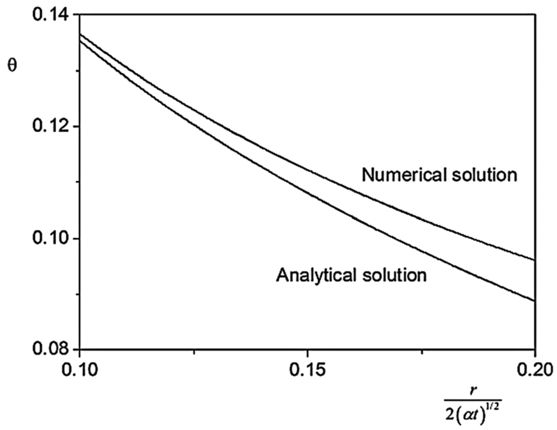

FIG. 4. Numerical and analytical results for the temperature distribution in the vicinity of a continuous line heat source.

Figure 4 shows the temperature distribution around a continuous line heat source when $r^2/4\alpha t$ is very small and at sufficiently long times. The results obtained from the numerical model are in good agreement with the analytical results, with a relative error less than 1% when $r/2(\alpha t)^{1/2}$ is smaller than 0.1.

The numerical simulations of the temperature field in the computational domain (Fig. 5) were used to determine the optimal spacing between cylinders. The work proceeded in these steps:

(1) Start with a guess for the spacing S.
(2) Solve Eq. (4), and find the peak temperature as the time increases.
(3) If the peak temperature is less than 1, calculate the new spacing as $S = S - \Delta S$.
(4) Repeat steps (2) and (3) until the peak temperature equals or exceeds 1.

Figure 6 shows the temperature distribution in the vicinity of time-dependent line heat sources when τ is 7.16×10^{-6}, which corresponds to $\alpha = 1.43 \times 10^{-6}$ m^2/s, D $= 1$ m, $t_c = 5$ s. When the spacing is large, the peak temperature is below 1, and this means that more space is available for heat deposition. When the spacing is too small, the peak temperature rises continuously. The optimum spacing between cylinders is at the intersection between these two limits of behavior when the maximum is $\theta = 1$.The resulting optimal spacing is reported in Fig. 7, which shows how S depends on the dimensionless group τ defined in Eq. (5).

IV. SCALE ANALYSIS

Figure 7 shows that when plotted log-log, the optimal spacing increases linearly as the dimensionless group τ increases. This trend can be anticipated based on scale analysis. From the conduction equation (2), the respective scales of the two terms are

$$\rho c \frac{\Delta T}{t} \sim k \frac{\Delta T}{L^2}. \tag{11}$$

This shows that the length scale of the heated zone L should increase as $(\alpha t)^{1/2}$. The spacing between cylinders S must be such that it matches the thermal diffusion scale that corresponds to the time scale of the heat deposition process,

$$S \sim (\alpha t_c)^{1/2} \tag{12}$$

or, in dimensionless terms,

$$\frac{S}{D} \sim \frac{(\alpha t_c)^{1/2}}{D} = \tau^{1/2}. \tag{13}$$

The dimensionless group $(\alpha t_c)^{1/2}/D$ accounts for the effect that the physical properties (α, t_c, D) have on the optimal

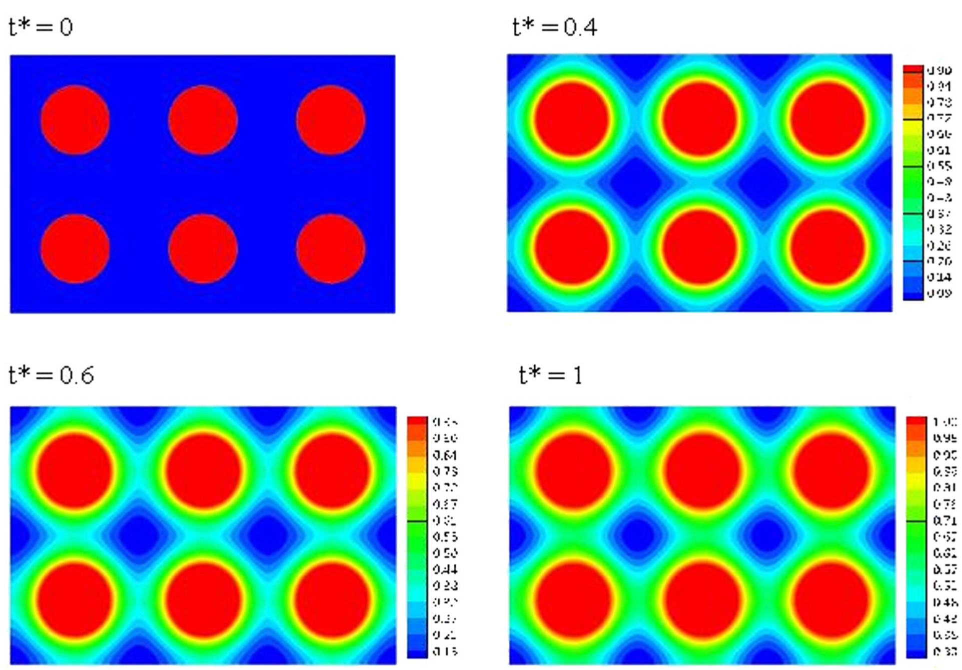

FIG. 5. (Color online) Contours of the dimensionless temperature field in a finite volume when $\tau = 0.16$, and the heat generation rate decays exponentially.

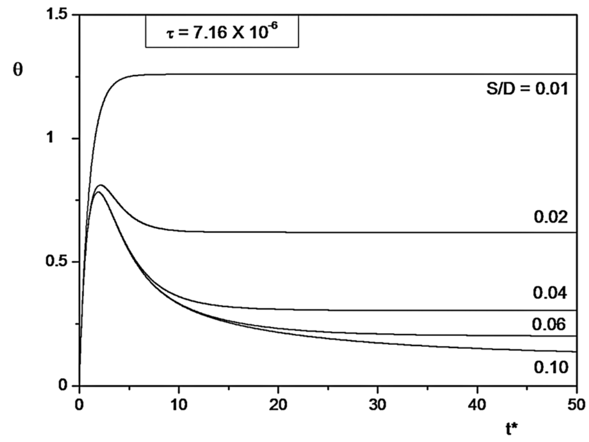

FIG. 6. The temperature distribution in the vicinity of a time-dependent line heat source with exponential behavior, showing the effect of the spacing S.

configuration of the design. According to Eq. (13), S/D should increase as $\tau^{1/2}$. Figure 7 shows that the agreement between scale analysis and numerical results is very good, qualitatively and quantitatively. The data of Fig. 7 are correlated with the expression suggested by Eq. (13), $S/D = C\tau^{1/2}$, where C is a factor of order 1, namely, $C \cong 2.7$.

The abscissa range in Fig. 7 covers the order of magnitude of $\tau^{1/2}$ that is representative. For example, in the case of heat exchanger pipes buried in soil, $\alpha \sim 0.56 \times 10^{-6}$ m^2/s, D $\sim$ 0.5 m, $t_c \sim$ 15 hours, and $\tau^{1/2} \sim 0.35$. In the case of nuclear waste buried in clay, the α value of clay is 0.133×10^{-6} m^2/s, D is of order 3 m, t_c is of order 10 years, and the order of magnitude of $\tau^{1/2}$ is 2.16.

V. STEPWISE TIME VARIATION

The optimal spacing represents the maximum heat deposition density in the volume. We applied the same method and the assumptions to the case when the embedded cylinders generate heat according to the stepwise behavior shown in Fig. 2,

$$q(t^*) = q_0, \quad t^* \le 1, \tag{14}$$

$$q(t^*) = 0, \quad t^* > 1. \tag{15}$$

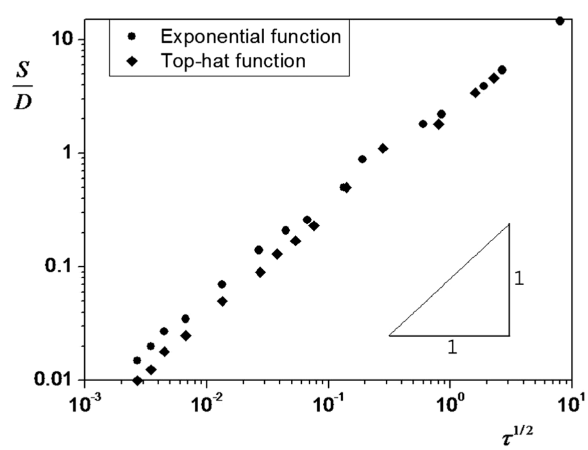

FIG. 7. The effect of the dimensionless group τ on the calculated optimal spacing.

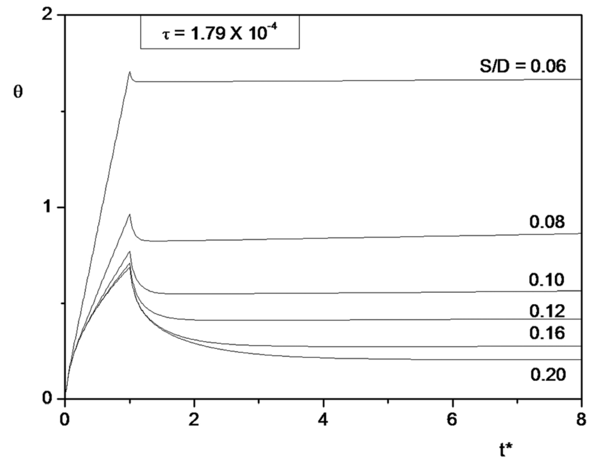

FIG. 8. The temperature distribution in the vicinity of a time-dependent line heat source with top-hat behavior, showing the effect of the spacing S.

The behavior of the temperature field (Fig. 8) is qualitatively the same as in Fig. 6. The optimal spacings have been added to Fig. 7, and their values and trend agree very well with the predictions based on scale analysis.

VI. TWO HEAT SOURCE SIZES

To deposit more heat in a finite volume, we can insert more cylinders between the heated zones, for example, in the subvolume B noted Fig. 1. We could insert a second-generation source or sink as shown in the upper part of Fig. 9, with a heat transfer rate scale q_1 in addition to q_0. The configuration now has two degrees of freedom, S/D and D_1/D. We

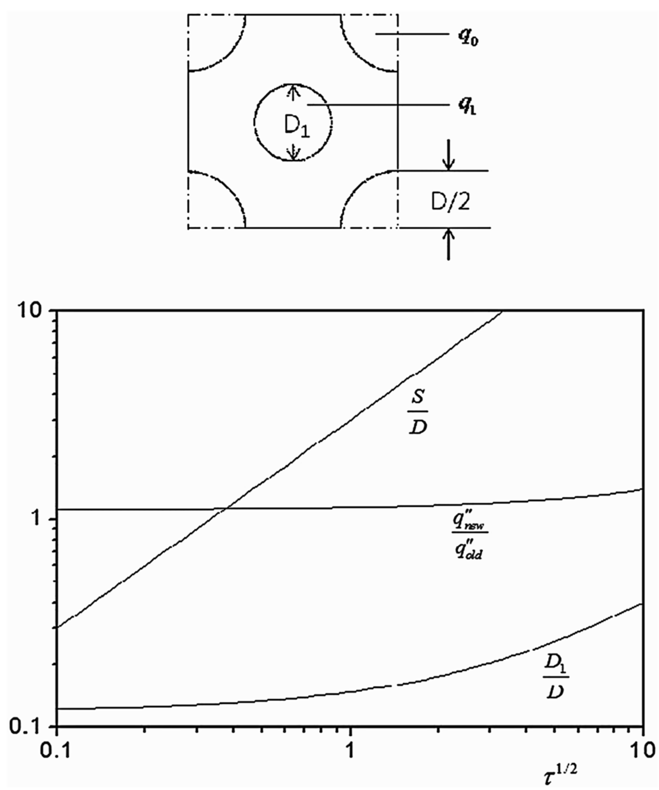

FIG. 9. The optimal geometry and performance of the configuration with heat sources of two sizes, relative to the configuration of Fig. 3.

optimized both and used the same numerical approach as in Sec. III. The objective was to find the best configuration $(S/D, D_1/D)$ and the corresponding heat transfer rate density $\left[q''_{new} = (q_1 + q_0)/(S+D)^2\right]$, relative to the preceding design $\left[q''_{old} = q_0/(S+D)^2\right]$. Note that that q''_{old} is the $D_1/D \to 0$ limit of q''_{new}. First, we fixed S/D at the value determined in Sec. V, and proceeded in these steps:

(1) Find q''_{new} by satisfying the condition that the peak temperature equals 1.
(2) If the new q''_{new} is larger than the previous q''_{new}, calculate the next cylinder diameter as $D_1 = D_1 + \Delta D_1$.
(3) Repeat steps (1) and (2) until the new q''_{new} is smaller than the old q''_{new}.

The resulting optimal values of D_1/D and q''_{new}/q''_{old} are reported in lower part of Fig. 9: when the second cylinder is inserted, the density of heat deposition in a finite volume increases.

Next, for the case of a time-dependent line heat source with exponential behavior, we allowed S/D to vary, and optimized both S/D and D_1/D to find the best configuration in a finite volume. We repeated the previous procedure as the spacing increases until q''_{new} does not increases. Figure 10 shows that the optimal spacing S/D continues to scale with $\tau^{1/2}$. In the case where $\tau^{1/2}$ is 0.40, which corresponds to $\alpha = 0.133 \times 10^{-6}$ m^2/s, D = 1 m, t_c is 13.5 days, we found that the optimal S/D is 1.27 and the optimal ratio between the two cylinder diameters is $D_1/D = 0.38$. Note that the spacings S/D are larger than the corresponding S/D values of Fig. 7, which is 1.1. In other words, when new sources or sinks are positioned among the old ones, the optimal spacing between the old ones increases. Compared to the old transfer rate density, the new heat transfer rate density increases by as much as 28%.

A question for future design work is to determine the optimal number of how many cylinders that can be packed on A when A and D are fixed (Fig. 1). In the case where $\tau^{1/2}$ is 0.75, we assumed that A is a square and $D/\sqrt{A}$ is 0.1, where $\sqrt{A}$ is the length scale of A. We simulated the temperature histories in four cases, each with a different number of

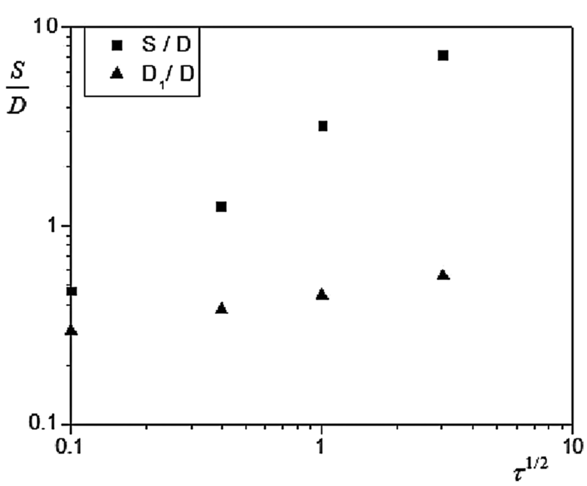

FIG. 10. The best configuration with heat sources of two sizes.

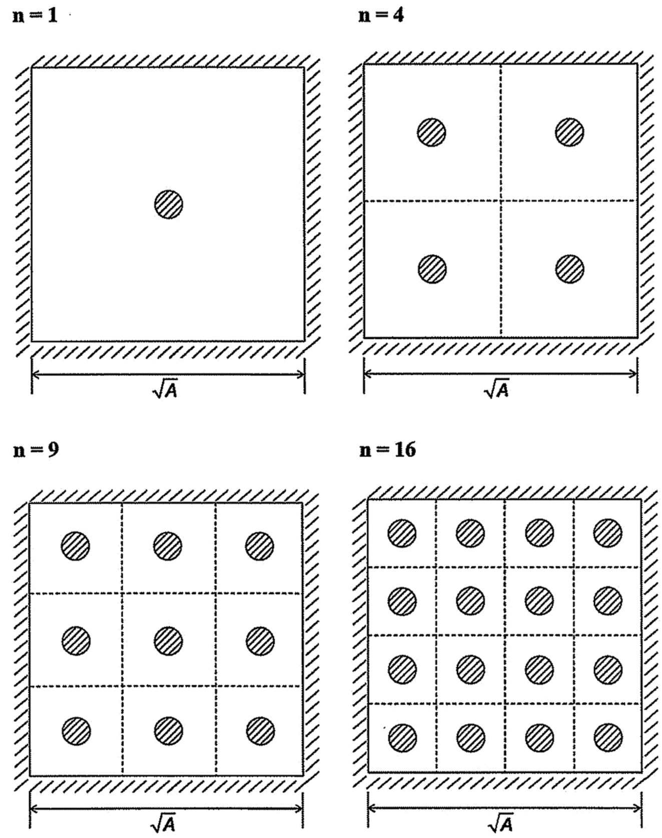

FIG. 11. Four arrangements for packing cylinders in a fixed volume.

cylinders such as Fig. 11. We found that when the number of cylinders is less than 9, *S*/*D* is larger than 2, and the maximal temperature is less than the allowable temperature. Otherwise, when the number of cylinders is 16, *S*/*D* is 1.5, the maximal temperature is larger than the allowable temperature. Using the optimal spacing of 2, as can be seen by referring to the previous results shown in Fig. 9, we find the optimal number of cylinders on A to be $\left[\sqrt{A/(S_{opt}+D)}\right]^2$, which yields n $\cong$ 11, the closest to which is n = 9 (Fig. 12).

VII. CONCLUSIONS

In this paper we solved the problem of optimizing the distribution of channels with heat transfer in a conducting medium by developing a numerical model to find the cylinder spacing that produces the maximum heating density within the volume without exceeding the temperature limit for the volume. From several numerical simulations for a time-dependent line heat source, we determined the optimal cylinder spacing as a function of the properties of the surrounding medium, the time scale of heat transfer process, and the dimensions of the configuration.

By using scale analysis we derived the relation between the optimal spacing and the time scale of the heat transfer process. We showed that S/D must be equal to $\tau^{1/2}$ in an order of magnitude sense, where τ is the dimensionless time scale of the process. This prediction agrees very well with the numerical results and provides the analytical form in which to correlate the numerical results. This conclusion

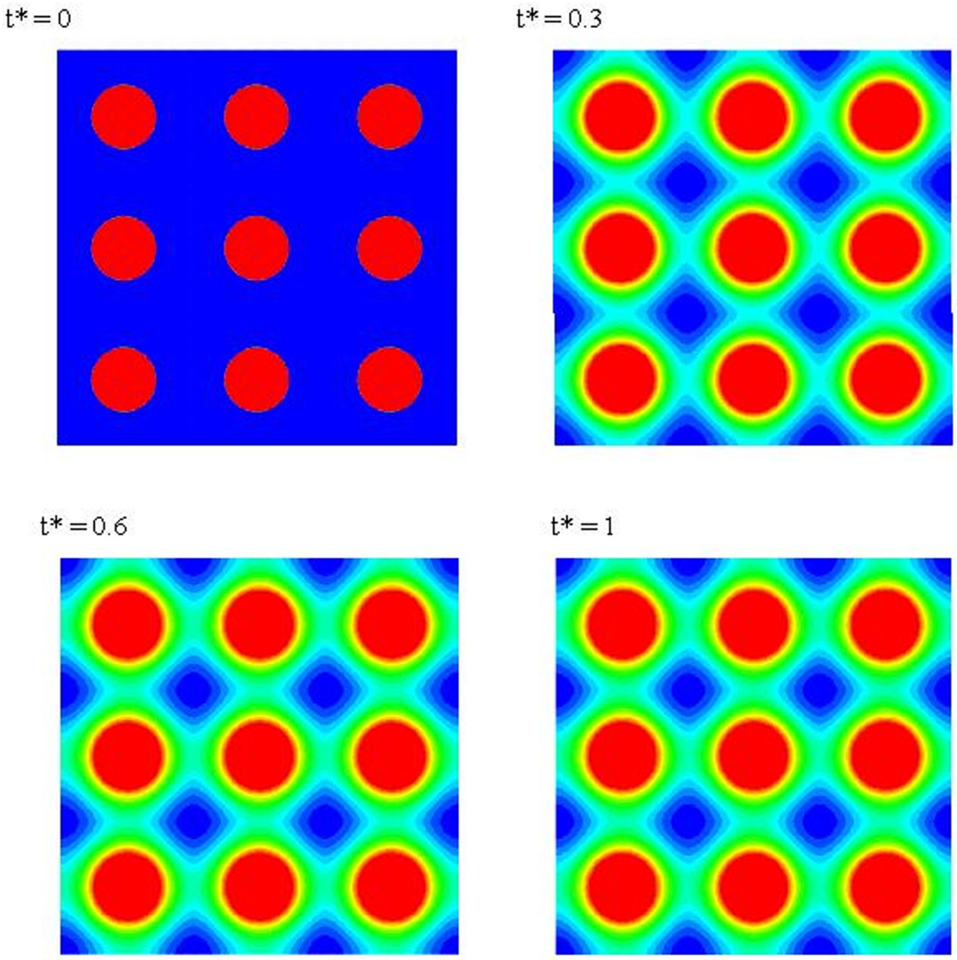

FIG. 12. (Color online) Contours of the dimensionless temperature field in the finite volume of Fig. 1 when $\tau^{1/2} = 0.75$ and $n = 9$.

holds for both heat transfer histories, exponential, and top hat. In addition, we extended the method to a packing of channels of two sizes (diameters and heat source strengths). Finally, through the use of multi-scale design techniques, we determined the optimum number of heat sources of two sizes within a finite volume.

ACKNOWLEDGMENTS

J.J. was supported by the Korea Science and Engineering Foundation (KOSEF) through the National Research Laboratory Program funded by the Ministry of Science and Technology (No. M10600000224O6J000022410). He also thanks Professor S. J. Kim of KAIST for his guidance and support. A.B. and S.L. were supported by a contract from the National Renewable Energy Laboratory (XXL-1-40325-01).

[1] B. Sanner, C. Karytsas, D. Mendrinos, and L. Rybach, Geothermics **32**, 579 (2003).
[2] T. Katsura, K. Nagano, and S. Takeda, Appl. Therm. Eng. **28**, 1995 (2008).
[3] H. Demir, A. Koyun, and G. Temir, Appl. Therm. Eng. **29**, 224 (2009).
[4] F. H. Cocks, *Energy Demand and Climate Change* (Wiley, Weinheim, 2009).
[5] A. Bejan and S. Lorente, Philos. Trans. R. Soc. B **365**, 1335 (2010).
[6] A. Bejan and S. Lorente, *Design with Constructal Theory* (Wiley, Hoboken, 2008).
[7] Y. S. Muzychka, Int. J. Therm. Sci. **46**, 245 (2007).
[8] A. Bejan, I. Dincer, S. Lorente, A. F. Miguel, A. H. Reis, *Porous and Complex Flow Structures in Modern Technologies* (Springer, New York, 2004).
[9] A. Bejan, *Shape and Structure: From Engineering to Nature* (Cambridge University Press, Cambridge, 2000), pp. 35–37.
[10] Y. Muzychka, Inter. J. Heat Mass Transfer **48**, 3119 (2005).
[11] A. Yilmaz, O. Buyukalaca, and T. Yilmaz, Inter. J. Heat Mass Transfer **43**, 767 (2000).
[12] C. Tannehill, A. Anderson, and H. Pletcher, *Computational Fluid Mechanics and Heat Transfer* (Taylor & Francis, Philadelphia, 1997).
[13] A. Bejan, *Heat Transfer* (Wiley, New York, 1993).